

Maximum Power Transfer Tracking in a Solar USB Charger for Smartphones

Abstract—Battery life of high-end smartphones and tablet PCs is becoming more and more important due to the gap between the rapid increase in power requirements of the electronic components and the slow increase in energy storage capacity of Li-ion batteries. Energy harvesting, on the other hand, is a promising technique that can prolong the battery life without compromising the users' experience with the devices and potentially without the necessity to have access to a wall AC outlet. Such energy harvesting products are available on the market today, but most of them are equipped with only a large battery pack, which exhibits poor capacity utilization during solar energy harvesting. In this paper, we propose and demonstrate that using a supercapacitor instead of a large capacity battery can be beneficial in terms of improving the charging efficiency, and thereby, significantly reducing the charging time. However, this is not a trivial task and gives rise to many problems associated with charging the supercapacitor via the USB charging port. We analyze the USB charging standard and commercial USB charger designs in smartphones to formulate an energy efficiency optimization problem and propose a dynamic programming-based online algorithm to solve the aforesaid problem. Experimental results show up to 34.5% of charging efficiency improvement compared with commercial solar charger designs.

I. INTRODUCTION

Smartphone sales have grown very rapidly since 2007 and reached sales volume of 144.4 million units as of 2012 [1]. State-of-the-art smartphones comprise high-performance application processors, high-bandwidth long term evolution (LTE) modems, and high resolution large sized displays that consume significant amount of power. However, there is only incremental progress in the battery capacity and technology. They are subject to volume and weight constraints that prohibit significant increase in battery capacity. Some smartphones do not even allow battery pack replacement. Thus, battery life is becoming a key concern for such power consuming products.

It is a good idea to utilize an energy harvesting smartphone charger to resolve the battery life issue. People often bring an external battery pack charged by a wall charger to relieve battery life problem for outdoor activities such as a camping and a hiking. However, energy harvesting chargers provide semi-permanent charging capability without looking for wall AC outlets unlike the external battery pack with a wall charger. Only some limited methods including solar energy harvesting or hand-crank generator among numerous harvesting methods are suitable for smartphones due to its large power demand. A number of commercial chargers using solar power have been developed. They focus on correct functionality, but system-level charging efficiency is not fully concerned.

Surprisingly, majority of low-cost smartphone solar chargers do not perform the maximum power point tracking [2], [3] of the solar panel. We exclude such a solar charger setup from discussion in this paper. Smartphone solar chargers that perform the maximum power point tracking rely on a large

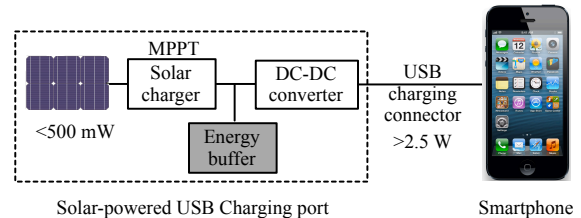
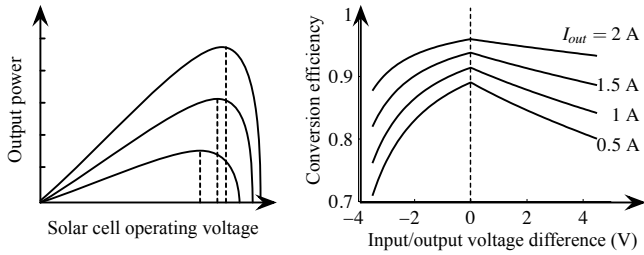


Fig. 1. USB-compatible solar charger architecture with an energy storage buffer.

capacity battery pack. It has benefit in that it can provide full USB charging current for the portable device. However, their solar panel size does not match with the battery pack capacity. For example, Figure 1 shows a typical setup of a solar-powered USB charger. Commercial USB chargers draw predetermined amount of current from USB charging port, and disconnect from the charging port if the amount is not supported [4], [5]. Thus, an built-in battery should be used as an energy buffer as shown in Figure 1. Ideally, the average power output of the solar charger should not be smaller than the charging power, which is not the case. As an alternative, USB charging current could be gracefully reduced depending on the change of irradiance intensity on the solar panel as a result of the maximum power point tracking (MPPT) [6], but such a feature is not defined in the USB charging port standard, and commercial charger chips in smartphones have no support for energy harvesting chargers. Therefore, the solar charger cannot provide 100% duty power to the smartphone. It has to be charged for a while to be able to support the USB charging current since small-sized solar panel is unable to support the USB charging power by itself. The battery collects a certain amount of energy from the solar panel using the MPPT while charging operation is stopped. The charging operation is resumed after the battery acquires a certain amount of energy. Such a stop-and-go operation continues. As the size of the battery is much bigger than the amount of energy to be collected for the stop-and-go operation, the battery state-of-charge (SOC) is always close to empty, which is very inefficient in terms of capacity utilization. The smartphone users will eventually end up charging the built-in battery pack from the wall AC outlet to utilize its full capacity. We could also try fully charging the built-in battery pack before the solar panel is exposed to the sun. However, such operational scenario makes the solar charger as a typical external battery pack. In addition, this would result in charging the two batteries sequentially and overall charging efficiency degradation due to cycle efficiency. This is not applicable to long-term outdoor activities either. One can resolve this contradiction of low capacity utilization by using a small size battery. However, small size batteries are subject to a low cycle



(a) The output power of a solar cell according to its operating voltage.

(b) Variation in converter efficiency according to input/output voltage difference

Fig. 2. The MPPT for energy harvesting devices.

efficiency due to low rate capability and a shorter battery life due to deep cycle operations during the stop-and-go operation.

In this paper, we propose to utilize a supercapacitor as an energy buffer in the USB-compatible solar charger for smartphones. We propose to use a supercapacitor as the energy buffer in USB solar chargers. A supercapacitor is superior in cycle life and efficiency compared with a battery, which makes a better candidate as an energy buffer and performing the maximum power transfer tracking (MPPT) of USB solar chargers. However, a new problem arises when we consider a supercapacitor as a buffer between the solar panel and the USB charging port. The terminal voltage variation of a supercapacitor causes degradation in associated power converter efficiency by offsetting the operating voltage and current from the optimal point. Thus, careful charge management such as the MPPT should be performed to maximize the chargers efficiency [7]. Determination of the supercapacitor capacitance and the SOC swing are also very crucial for the optimal solar charger control.

We analyze the USB charging standard and commercial designs of USB charger in the portable device, and address energy efficiency problems in utilizing solar power and supercapacitor in such environment. We finally propose a dynamic programming based online charging algorithm for proposed battery-less USB solar chargers. The proposed algorithm is fully compatible with the USB charging standard that makes it work applicable without modifications in commercial smartphones.

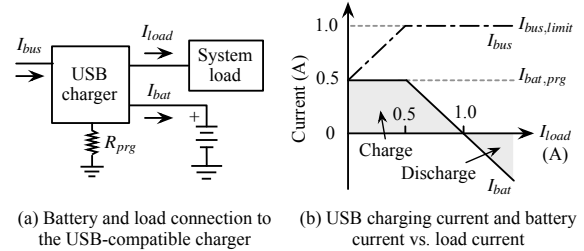
II. BACKGROUND

A. Maximum Power Transfer Tracking and Conversion Efficiency

The V-I curve of a solar panel is generally far from an ideal battery, and thus it requires careful management to achieve high energy efficiency as shown in Figure 2(a). The output power deviates significantly according to the operating voltage, current, and solar irradiance. The MPPT is a widely used technique that tracks the optimal operating point of a solar panel according to changing solar irradiance [6].

The power conversion loss of a power converter plays a significant role in overall system energy efficiency. The energy efficiency of the power converters is a varying value that can be expressed as a function of input voltage, output voltage, and output current.

$$\eta(V_{in}, V_{out}, I_{out}) = \frac{P_{out}}{P_{in}} = \frac{P_{in} - P_{loss}}{P_{out}}. \quad (1)$$



(a) Battery and load connection to the USB-compatible charger

(b) USB charging current and battery current vs. load current

Fig. 3. Programmable charger operation.

The variation of the conversion efficiency is more significant when considering a supercapacitor. The terminal voltage of a supercapacitor varies linearly according to its SOC, which affects the efficiency of the associated power converters that varies significantly as shown in Figure 2(b). Therefore, it is essential to perform the MPPT that maximizes actual energy delivered from the energy harvesting device to the energy storage considering both power generation and conversion efficiency [7].

B. USB Charging Standard

USB charging specification is a *de facto* standard for charging smartphone batteries. However, it is designed for power sources such as wall AC outlet and large external batteries, and it does not support energy harvesting chargers that often fail to meet the USB charging port requirement according to surrounding environment. Restrictions on the input voltage and current of the commercial USB charger chip in portable devices make it hard to enhance system-level charging efficiency of solar chargers using the MPPT. Solar chargers require continuous control of the charging current that allows an arbitrary current value in the USB for performing the MPPT of the solar cell, which is true for a medium- to large-scale solar panels [6]. However, commercial USB compatible charger chips in smartphones do not allow room for continuous control of charging current [4], [5].

A more detailed look of a USB-compatible solar charger is shown in Figure 3. Battery charge current $I_{bat,prg}$ is programmed by a resistor R_{prg} as $I_{bat,prg} = k/R_{prg}$, which is usually fixed. The USB charging current I_{bus} is defined as the input current of portable device side charger as shown in Figure 3(a). The value of I_{bus} is increased as the load current I_{load} increases. The maximum value of I_{bus} is fixed to $I_{bus,limit}$, so that I_{bat} has to be decreased if I_{bus} is clamped. Battery is discharged if I_{bus} only cannot support I_{load} . They are disconnected from the USB charging port or abruptly reduce I_{bus} when the USB charging port is unable to supply I_{bus} at any moment during this operation. The USB charging port should support at least 0.5 A for standard downstream port (SDP), and 1.5 A for charging downstream port (CDP) and dedicated charging port (DCP). It is not defined in the standard how the portable device side charger should handle when the power output of the charging port is insufficient. Our observation shows that many portable device side charger reduces the input current limit to a predefined value to prevent failure in a “badly designed” charging port. The only feasible method for the MPPT without modifying commercial smartphones is stop-and-go based control.

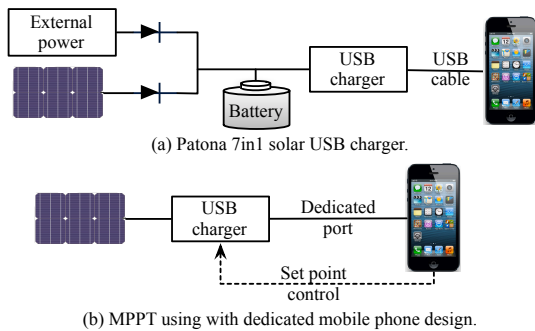


Fig. 4. Previous solar USB charger topology.

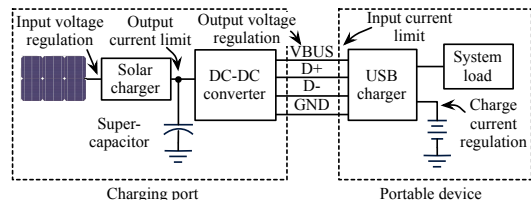


Fig. 5. Proposed USB-compatible solar charger architecture with a supercapacitor buffer.

USB stop-and-go operation incurs some time and energy overhead. USB charging standard defines charging port detection algorithm that distinguishes SDP, CDP, and DCP [8]. The detection algorithm running on portable device side sequentially performs VBUS detect, data contact detect, primary detect, secondary detect, and ACA detect to determine the charging port type. This typically takes several hundreds of milliseconds, which becomes minimum overhead of stop-and-go control. In this paper, we consider the time overhead only, which is constant once the system configuration is fixed. We assume the energy overhead of stop-and-go is negligible considering relatively large USB charging power.

C. Existing Solar Charger Designs

There already are commercial chargers available in the market. The simplest and cheapest solution is connection of a solar panel to the smartphone with diodes such as Patona 7in1 solar charger for smartphones, which is shown in Figure 4(a) [2]. However, this design has shortcomings in that cannot perform the MPPT, and discards solar energy when solar panel output power is below a threshold. Solar chargers with a DC-DC converter may perform the MPPT. A recent work has explored the possibility of using the CPU in mobile phones as a microcontroller for performing the MPPT [3]. The solar panel is connected to the mobile battery via a DC-DC converter without any built-in energy storage in the design as shown in Figure 4(b). However, it requires another charging port from the smartphone besides the USB interface, which is not the usual case for general smartphones, because it performs continuous control of charging current. We need an energy buffer as shown in Figure 1 to perform energy efficiency optimization such as the MPPT while meeting USB charging standard. However, no extensive work has been performed on energy efficient design and control of USB-compatible solar chargers. Existing solar chargers for smartphones generally rely on large capacity Li-ion batteries [9], [10] and are subject to problems as we discussed in Section I.

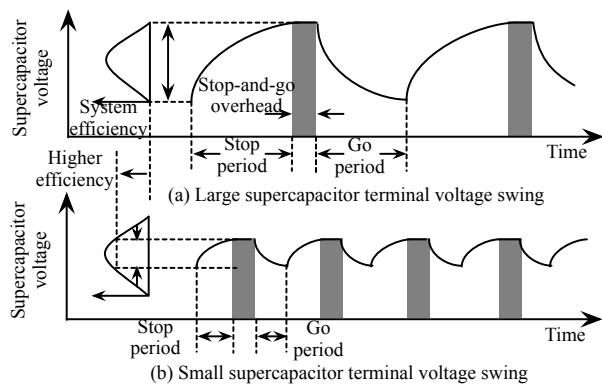


Fig. 6. Trade-off relationship between converter efficiency loss and USB stop-and-go overhead.

III. PROPOSED SOLAR CHARGER DESIGN AND CONTROL ALGORITHM

A. Solar Cell-Supercapacitor Hybrid Architecture

In this paper, we propose to use a supercapacitor as an energy buffer for performing the MPPT in USB-compatible solar charger for smartphones. Figure 5 shows the proposed architecture of the conventional charger. The energy capacity of the supercapacitor is much smaller than built-in battery packs used in commercial products because it is not for long-term energy storage but used as an intermediate buffer to perform the MPPT. Usage of supercapacitor induces new issues including supercapacitor SOC change, which affects overall system efficiency. The conversion efficiency of three converters in Figure 5 varies according to supercapacitor terminal voltage change as shown in Figure 2(b). If the supercapacitor terminal voltage is maintained too low or too high, there will be higher conversion loss in the converters, and less energy will be delivered to the mobile device. There exists the optimal supercapacitor terminal voltage that minimizes the conversion loss in the converters. We thus intend to find the optimal supercapacitor terminal voltage to minimize the conversion loss and thus maximize the charging power to the smartphone. The USB charging standard leaves stop-and-go control as the only option as discussed in Section II-B. The terminal voltage of the supercapacitor should swing up and down the optimal value due to stop-and-go control as shown in Figure 6. The conversion loss could be large depending on the control of stop-and-go control. For example, excessively coarse-grain control would make the solar charger and DC-DC converter in Figure 5 and operate it in low efficiency region for a significant amount of period as shown in Figure 6(a). Fine-grain stop-and-go control enables the associated converters to operate more in the high-efficiency region, but the overall charging process would be inefficient due to the large stop-and-go overhead as shown in Figure 6(b).

B. Charging Efficiency Maximization Problem Formulation

The objective of the control algorithm is to maximize the average charging power $\overline{P_{bat}}$ for the battery in a mobile device. Average charging power is average battery input power over the total charging time compensated by non-idealistic battery

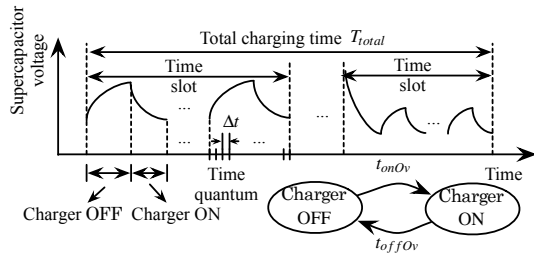


Fig. 7. Terms for charging efficiency-optimal SOC swing subproblem.

characteristics such as internal resistance and rate capacity effect. The objective function is formally given as

$$\overline{P_{bat}} = \frac{1}{T_{total}} \sum_{n=1}^{N_{total}} P_{bat,eff}[n] \Delta t, \quad (2)$$

where T_{total} is the charging time, $P_{bat,eff}[n]$ is the actual charging power of the battery at time quantum q_n that allows for non-ideal battery characteristics such as limited rate capacity capability [11], Δt is the length of the time quantum, and N_{total} is the number of the time quanta that satisfy $T_{total} = N_{total} \cdot \Delta t$, respectively. This objective is equivalent to charging time minimization as charging time will be minimized if the average charging power is maximized. The detailed terms are given in Figure 7.

Given values for the problem are solar irradiance G , system load current I_L , supercapacitor SOC, SOC_{cap} , and battery SOC, SOC_{bat} at the beginning of a time slot. Making predictions on future G and I_L would benefit for stationary solar power plants and rooftop solar panels etc., which are located in a place that can be free from fast environmental condition change as much as possible. However, prediction of G and I_L is limited for a portable smartphone solar charger. Load current of semiconductor components in a smartphone indeed contains high frequency components, but they are filtered out by bulk capacitors in the power converters. Therefore, the current waveform at the charger input does not contain dominant high frequency components over 1 kHz. Thus, we consider an online algorithm based on the currently measured current. We assume that the solar irradiance and load demand do not change within a time slot, which is not longer than a few seconds. The power conversion efficiency of the solar charger, DC-DC converter, and USB charger influences the overall charging efficiency significantly. The conversion efficiency is well modeled as a function of its input voltage, output voltage, and output current [7]. Functions $\eta_{solar}(V_{in}, V_{out}, I_{out})$, $\eta_{DC}(V_{in}, V_{out}, I_{out})$, and $\eta_{USB}(V_{in}, V_{out}, I_{out})$ denote conversion efficiency of the solar charger, DC-DC converter, and USB charger, respectively.

The control knob for optimization is on/off control of the USB charging for each time quantum. We define a variable USB to accommodate the control knob. Variable USB has one of the following four charging decisions, ‘‘ON’’, ‘‘OFF’’, ‘‘TURNING ON’’, and ‘‘TURNING OFF’’. The output of the control algorithm is the energy optimal on/off charging schedule, that is $USB[n]$ for every time quantum q_n .

C. Solution Method

We propose an online algorithm that follows dynamic load and solar irradiance change at runtime. Power generation of the solar cell depends on the weather conditions, obstacles, and direction of the solar panel, which dynamically change during runtime. The proposed method is an online discrete time approach that performs Algorithm 1 every time slot. Algorithm 1 finds the optimal charge scheduling using dynamic programming. Each time quantum becomes the decision stage of the dynamic programming algorithm, and the algorithm determines the charging state decision USB . We first formulate the problem $Swing(V_{cap,N}, N)$ that finds charging efficiency-optimal schedule (maximized (2)) that makes the supercapacitor voltage at time $T = N \cdot \Delta t$ to be $V_{cap,N}$. We apply dynamic programming to solve $Swing(V_{cap,N}, N)$ so that $Swing(V_{cap,N}, N)$ should satisfy the optimal substructure property in order to exploit dynamic programming.

The optimal substructure property of $Swing(V_{cap,N}, N)$ problem: Suppose a sequence of $\tau_N = \{(V_{cap}[n], usb[n]) \mid 1 \leq n \leq N\}$, is the optimal solution of $Swing(V_{cap,N}, N)$. A subsequence $\tau_M = \{(V_{cap}[m], usb[m]) \mid 1 \leq m \leq M \text{ where } M < N\}$, is the optimal solution of $Swing(V_{cap,M}, M)$, a subproblem of $Swing(V_{cap,N}, N)$.

Proof: There exists a different sequence υ_M that exhibits higher charging efficiency than τ_M if the subsequence τ_M is not the optimal solution for $Swing(V_{cap,M}, M)$. This implies that a sequence that is a concatenation of υ_M and the tail of τ_N should exhibit a higher efficiency than τ_N . This contradicts to the assumption that τ_N is the optimal solution, and thus, the optimal substructure property is proved. ■

Algorithm 1 explains how SOC swing should be managed to achieve high charging efficiency. We build a two-dimensional table, $T_{SOC,n}[V_{cap}, USB]$, for each time quantum q_n using dynamic programming. Table indexes are quantized value of V_{cap} and the charging decision USB . The entry value of $T_{SOC,n}[V_{cap}, USB]$ is the expected battery SOC, SOC_{bat} , at time quantum $q_n + 1$ when supercapacitor voltage at time quantum q_n is V_{cap} , and selected charging decision is USB . Algorithm 1 shows the SOC swing determination algorithm aiming at the maximum efficiency. The algorithm initializes the first table such that $T_{SOC,0}(V_{cap,0}, USB_0) \leftarrow SOC_{bat,0}$ and fill the rest of the tables using dynamic programming. Function $nextValue(G, I_L, V_{cap}, nextStat)$ calculates the supercapacitor voltage and battery SOC for the next time slot depending on $nextStat$ using the component models discussed in Section II-A. We perform backtracing to obtain the optimal charging schedule after table construction is finished. The selection of (V_{cap}, USB) pair in $T_{SOC,N}$ to start backtracing is very important. Greedy approach per time slot that picks (V_{cap}, USB) pair with the highest battery SOC value in $T_{SOC,N}$ is not the globally optimal as it results in discharging the supercapacitor buffer as much as possible within a time slot to maximize the smartphone battery charging power. The algorithm should charge the supercapacitor up to certain voltage level at the next time slot, which is energy inefficient. Thus, we pick appropriate $(V_{cap,opt}, USB_{opt})$ in $T_{SOC,N}$ to start backtracing by Algorithm 2 offline. We construct a look up table by offline

Algorithm 1: Optimal supercapacitor SOC swing algorithm.

Input: $G, I_L, SOC_{bat,0}, V_{cap,0}$
Output: Charging schedule $USBStat[n]$ for every n

```

1 for  $n = 0 \rightarrow N$  do
2   for  $\forall(V_{cap}, USB)$  do
3      $T_{SOC,n}(V_{cap}, USB) \leftarrow -1$ 
4  $T_{SOC,0}(V_{cap,0}, \forall USB) \leftarrow SOC_{bat,0}$ 
5 for  $n = 0 \rightarrow N - 1$  do
6   for  $\forall(V_{cap}, USB)$  pair do
7     if  $T_{SOC,n}(V_{cap}, USB) = -1$  then
8       continue
9     if  $USB = OFF$  then
10      for  $nxtStat = OFF, TURNING ON$  do
11         $(V_{cap,nxt}, SOC_{bat,nxt}) \leftarrow$ 
12           $nextValue(G, I_L, V_{cap}, nxtStat)$ 
13        if  $SOC_{bat,nxt} > T_{SOC,n+1}(V_{cap,nxt}, nxtStat)$  then
14           $T_{SOC,n+1}(V_{cap,nxt}, nxtStat) \leftarrow SOC_{bat,nxt}$ 
15           $Prev_{n+1}(V_{cap,nxt}, nxtStat) \leftarrow (V_{cap}, USB)$ 
16      else if  $USB = TURNING ON$  then
17         $nxtStat = ON$ 
18         $(V_{cap,nxt}, SOC_{bat,nxt}) \leftarrow$ 
19           $nextValue(G, I_L, V_{cap}, nxtStat)$ 
20        if  $SOC_{bat,nxt} > T_{SOC,n+1}(V_{cap,nxt}, nxtStat)$  then
21           $T_{SOC,n+1}(V_{cap,nxt}, nxtStat) \leftarrow SOC_{bat,nxt}$ 
22           $Prev_{n+1}(V_{cap,nxt}, nxtStat) \leftarrow (V_{cap}, USB)$ 
23      else if  $USB = ON$  then
24        for  $nxtStat = ON, TURNING OFF$  do
25           $(V_{cap,nxt}, SOC_{bat,nxt}) \leftarrow$ 
26             $nextValue(G, I_L, V_{cap}, nxtStat)$ 
27          if  $SOC_{bat,nxt} > T_{SOC,n+1}(V_{cap,nxt}, nxtStat)$  then
28             $T_{SOC,n+1}(V_{cap,nxt}, nxtStat) \leftarrow SOC_{bat,nxt}$ 
29             $Prev_{n+1}(V_{cap,nxt}, nxtStat) \leftarrow (V_{cap}, USB)$ 
30          else if  $USB = TURNING OFF$  then
31             $nxtStat = OFF$ 
32             $(V_{cap,nxt}, SOC_{bat,nxt}) \leftarrow$ 
33               $nextValue(G, I_L, V_{cap}, nxtStat)$ 
34            if  $SOC_{bat,nxt} > T_{SOC,n+1}(V_{cap,nxt}, nxtStat)$  then
35               $T_{SOC,n+1}(V_{cap,nxt}, nxtStat) \leftarrow SOC_{bat,nxt}$ 
36               $Prev_{n+1}(V_{cap,nxt}, nxtStat) \leftarrow (V_{cap}, USB)$ 
37  $V_{cap,opt} \leftarrow LUT_{V_{cap}}(G, I_L)$ 
38  $USB \leftarrow max_{arg} USB(T_{SOC,N}(V_{cap,opt}, USB))$ 
39 for  $n = N \rightarrow 0$  do
40    $(V_{cap}, USB) = Prev_n(V_{cap}, USB)$ 
41    $USBStat[n] \leftarrow USB$ 

```

characterization in the form of $V_{cap,opt} = LUT_{V_{cap,opt}}(G, I_L)$. The algorithm sweeps V_{cap} and calculates the value that minimizes the conversion loss from the solar panel to the mobile device. Backtracing from $T_{SOC,N}(V_{cap,opt}, USB_{opt})$ to $T_{SOC,0}(V_{cap,0}, USB_0)$ gives the optimal charging schedule.

IV. EXPERIMENTS

We show the efficacy of the proposed design and online charging algorithm compared with commercial chargers with the MPPT capability. We evaluate the performance of the proposed design and the online charging algorithm on most general setups. The size of the solar panel used for experiments

Algorithm 2: Offline algorithm for finding $V_{cap,opt}$, which is starting point of backtracing.

Input: Solar irradiance G , Load current I_L
Output: Backtracing starting voltage $V_{cap,opt}$

```

1  $I_{bat,max} \leftarrow 0$ 
2 for  $\forall_{quantized}(V_{cap}, G, I_L)$  do
3    $(V_{solar}, I_{solar}) \leftarrow MPPT(G, V_{cap})$ 
4    $P_{solar} \leftarrow V_{solar} \cdot I_{solar}$ 
5    $I_{solar,out} \leftarrow find_I(\eta_{solar}(V_{solar}, V_{cap}, I) \cdot P_{solar} = V_{cap} \cdot I)$ 
6    $I_{DC,in} \leftarrow I_{solar,out}$ 
7    $P_{DC,in} \leftarrow V_{cap} \cdot I_{DC,in}$ 
8    $I_{DC,out} \leftarrow find_I(\eta_{DC}(V_{cap}, V_{USB}, I) \cdot P_{DC,in} = V_{USB} \cdot I)$ 
9    $I_{USB,in} \leftarrow I_{DC,out}$ 
10   $P_{USB,in} \leftarrow V_{USB} \cdot I_{USB,in}$ 
11   $I_{bat} \leftarrow find_I(\eta_{USB}(V_{USB}, V_{bat}, I_L, I) \cdot P_{USB,in} = P_L + V_{bat} \cdot I)$ 
12  if  $I_{bat} > I_{bat,max}$  then
13     $I_{bat,max} \leftarrow I_{bat}$ 
14     $LUT_{V_{cap}}(G, I_L) \leftarrow V_{cap}$ 

```

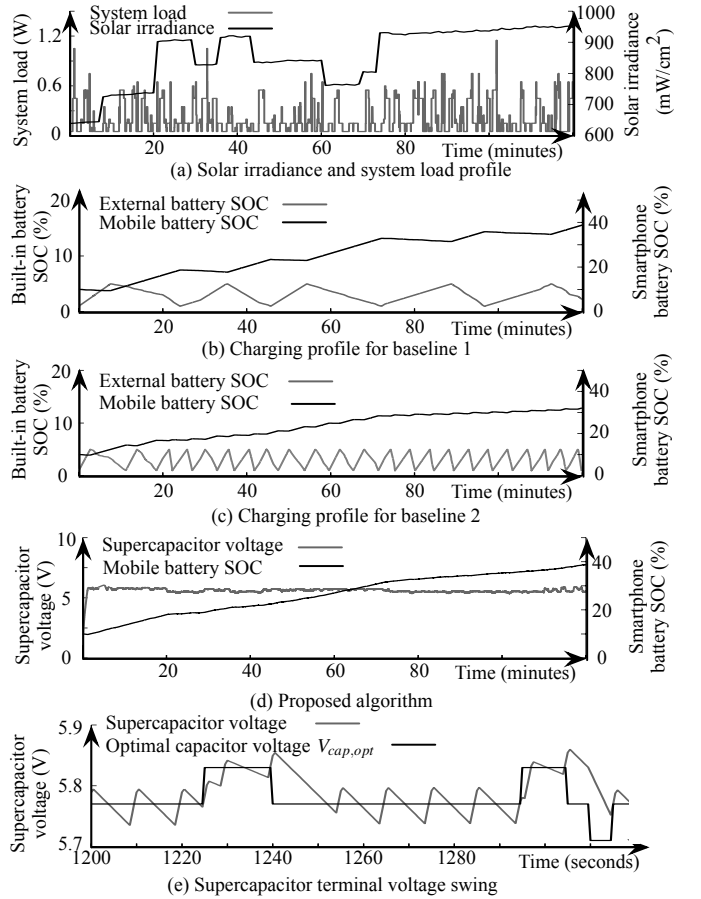


Fig. 8. Comparison of battery charging process over time.

is comparable to the size of representative commercial solar chargers for smartphones and tablets. We assume a 29.2 cm by 16.8 cm solar panel capable of producing 2104 mW at 100 mW/cm². The solar irradiance is a time varying value but generally is at most 100 mW/cm² measured in Hawaii [12]. The solar irradiance changes according to the direction of the solar panel and nearby obstacles that shade the solar panel. We assume a situation such as a tracker using a solar charger

attached on the backpack, and the perceived solar irradiance changes according to direction of walking. The smartphone battery is an Li-ion battery with capacity of 1500 mAh. The smartphone system load changes according to usage pattern of the users and application behaviors.

We compare the proposed architecture and algorithm with two baselines. The first baseline is the solar charger with a large built-in battery pack of 2000 mAh capacity in the charger. Comparison is made for the steady-state long-term outdoor usage cases, and we assume zero initial SOC for all the setups. The solar panel is controlled by the MPPT algorithm to maximize its output power. We perform stop-and-go operation for baselines as explained in Section 1. The second baseline is a solar charger with a small buffer battery, and all the other components in the experimental setup are kept the same. We show the efficacy of our proposed algorithm for various sizes of supercapacitors.

Figure 8 shows the comparison between the baselines and proposed algorithm for two hours of charging. Figure 8(a) shows the profile of solar irradiance and system load. Solar irradiance profile is generated based on data measured in Hawaii by NREL [12] and modified to reflect changes of the solar panel direction and shading. We use a synthetic smartphone load with the maximum value of about 1.5 W. Figure 8(b) shows charging process of the first baseline. The built-in battery pack of 1.5 Ah capacity is charged from the solar panel until its SOC reaches a threshold. The charger circuitry determines the open circuit voltage of the built-in battery and discharges it when it has accumulated enough charge. The threshold value generally small, so we assume it to be 5% in our setup. Figure 8(c) shows charging process of the second baseline, which uses much smaller battery than the first baseline, 300 mAh. We compared the proposed method with baselines when there is change in surrounding environment such as solar irradiance and system load for more direct comparison.

Figure 8(d) shows the proposed algorithm that uses a supercapacitor as a buffer. Size of the supercapacitor buffer used in the proposed setup is 10 F, which has a reasonably small form factor and enough capacitance to avoid large fluctuation in the terminal voltage as shown in Figure 1. Two baselines charge the built-in battery up to 28.7% and 22% of the full capacity, respectively. The proposed algorithm charges up to 29.6% of full capacity, which is 3.14% larger than the first baseline and 34.5% larger than the second baseline. Overall charging efficiency of the first baseline is comparable to the proposed technique using the supercapacitor buffer. This is because large capacity battery used in the first baseline exhibits high rate capability and thus high cycle efficiency. However, such a large capacity battery does not match with a small solar panel size as well as higher cost and heavier weight, and it stays empty for most of the time. Figure 8(e) shows a detailed result of proposed algorithm. The voltage swing follows $V_{cap,opt}$ obtained from Algorithm 2. Table I summarizes Figure 8 and shows results with various different supercapacitor capacitance. The result shows that larger capacitor shows higher solar charging efficiency because it suffers less from terminal voltage fluctuation and better tracks $V_{cap,opt}$.

TABLE I
CHARGED ENERGY IN 2 HOURS, AVERAGE CHARGING POWER, AND V_{cap} STANDARD DEVIATION.

		Charged energy in 2 hours (J.)	Average charging power (mW)	V_{cap} standard deviation (V)
Baseline 1		6044	0.839	N/A
Baseline 2		4633	0.644	N/A
Proposed	5 F	6213	0.863	0.0823
	10 F	6234	0.867	0.0492
	20 F	6255	0.869	0.0438

V. CONCLUSIONS

This is the first work that systematically optimize the charging efficiency of solar charger for smartphones without modifying the existing smartphone charger circuitry. We analyze the USB charging standard and commercial USB-compatible battery charger chips equipped in smartphones to explore the possibility of charging efficiency optimization while meeting the USB charging standard. We propose a stop-and-go charging procedure, which is the only feasible way to perform optimization without modifying the legacy smartphone designs. This paper introduces a USB-compatible solar charger for smartphones using supercapacitor as the energy buffer to support the maximum power transfer tracking (MPPT). Most commercial solar chargers rely on a large-capacity built-in battery. Such a solar charger with a built-in battery has drawbacks in many aspects including cycle life, weight, volume, cost, etc., as well as low solar charging efficiency. Instead, we propose to use a supercapacitor as an energy buffer and derive an dynamic programming-based online charging control algorithm that effectively maximizes the solar charging efficiency. Experiments show up to 34.5% improvement in solar charging efficiency over small size built-in batteries and 3.14% improvement to large built-in batteries even with small-size supercapacitors.

REFERENCES

- [1] Gartner Inc., *Gartner Says Worldwide Sales of Mobile Phones Declined 2 Percent in First Quarter*, 2012.
- [2] C. Schuss and T. Rahkonen, "Photovoltaic (PV) energy as recharge source for portable devices such as mobile phones," in *Conference of FRUCT Association*, 2012.
- [3] —, "Use of mobile phones as microcontrollers for control applications such as maximum power point tracking (MPPT)," in *MELECON*, 2012.
- [4] Texas Instruments, *BQ24072 USB-Friendly Li-Ion Battery Charger and Power-Path Management IC*, 2011.
- [5] Linear Technology, *LTC4160 - Switching Power Manager with USB On-The-Go And Overvoltage Protection*.
- [6] T. Esmar, J. Kimball, P. Krein, P. Chapman, and P. Midya, "Dynamic maximum power point tracking of photovoltaic arrays using ripple correlation control," *IEEE T. on Power Electronics*, 2006.
- [7] Y. Kim, N. Chang, Y. Wang, and M. Pedram, "Maximum power transfer tracking for a photovoltaic-supercapacitor energy system," in *ISLPED*, 2010.
- [8] USB Implementers Forum, "Battery charging specification revision 1.2," 2010.
- [9] P. English, A. Viejo, and S. R. Brimmer, "Solar chargeable battery for portable devices," *United States Patent Application Publication*, 2010, US 2010/0207571 A1.
- [10] P. English, A. Viejo, R. E. Sanett, and S. R. Brimmer, "Stand alone solar battery charger," *United States Patent Application Publication*, 2011, US 2011/0199040 A1.
- [11] D. Doerffel and S. A. Sharkh, "A critical review of using the peukert equation for determining the remaining capacity of lead-acid and lithium-ion batteries," *Journal of Power Sources*, 2006.
- [12] Solar Radiation Research Laboratory, NREL, *Current Irradiance and Meteorological Conditions*, http://www.nrel.gov/midc/srrl_bms, 2013.